INFLUENCE OF THE BODY ON HEAD ROTATIONAL ACCELERATION IN MOTORCYCLE HELMET OBLIQUE IMPACT TESTS

Mazdak Ghajari [a], Steffen Peldschus[b], Ugo Galvanetto[c], Zahra Asgharpour[b], Lorenzo Iannucci [a]

[a] Imperial College London, Department of Aeronautics, South Kensington Campus, London SW7 2AZ, UK
[b] Ludwig-Maximilians University, Institute of Legal Medicine, Nussbaumstr. 26, Munich 80336, Germany
[c] Padova University, DCT, Via Marzolo 9, 35131 Padova, Italy

ABSTRACT

The Finite Element (FE) method has been used to study full-scale oblique impacts of a motorcycle helmet. For these impacts, an elaborate FE model of the human body was employed. The results were compared to the results of the same impacts but by using the detached head of the body. It has been found that the presence of the body influences the head rotational acceleration components (up to 40% for the simulated impact configuration). On the basis of the equations of general three-dimensional motion of a rigid body, it is shown that this influence can be taken into account in detached head impact tests through modifying the inertia matrix of the head. For a severe oblique impact, the modified inertia was calculated and applied to the head. The head rotational acceleration components predicted by using the modified detached head were in good agreement with those obtained from full-scale oblique impacts.

Keywords: Helmets, Human Body, Full Scale Tests, Drop Tests, Finite Element Method

IN A NUMBER OF MOTORCYCLE ACCIDENTS, the body impacts the opposite object at a shallow angle (Richter, et al., 2001), which implies that the impact velocity has a component tangential to the impact surface in addition to a normal component. These impacts are called oblique. Conversely, in normal impacts, the impact velocity has only a normal component. According to current helmet standards, the energy absorption capacity of safety helmets are measured in normal impact tests (Ghajari, et al., 2008). The helmet is coupled with a headform and dropped onto a flat anvil. The helmet pass the test if the linear acceleration of the headform measured at its centre of gravity (C.G.) is lower than a given limit.

The head rotational acceleration, however, is believed to be an important cause of head injuries. Holbourn (1943) believed that rotational acceleration applied to the head, with or without direct impact, results in shear and tensile strains in the brain and bridging veins, which cause haematoma and diffuse axonal injury (DAI). Gennarelli (1983) concluded that subdural haematoma was mainly due to short duration and high amplitude rotational accelerations, while DAI was mainly due to long duration and low amplitude rotational accelerations. A combination of a 10 krad/s^2 rotational acceleration and a 100 rad/s maximum change in the rotational velocity of the head has been proposed as a limit for DAI (Margulies and Thibault, 1992).

There is an oblique impact test in some helmet standards, such as British (BS6658, 1985) and UN ECE standards (2002). The aim of this test is to assess the forces caused by friction at the helmet/anvil interface. The ECE 22.05 standard has two test methods for oblique impact testing helmets. In method A, which is simpler than method B, a headform fitted with the helmet is dropped onto a 15° inclined anvil at a 8.5 m/s impact speed. The anvil is covered with an abrasive paper to increase the friction at the helmet/anvil interface. During the tests, the tangential force (F_T) and its integral with time (J, impulse) are measured. The pass criteria are $F_T < 3.5$ kN and $J < 25$ N.s.

In real world motorcycle accidents, the body always interacts with the head. The influence of this interaction on head and helmet responses has been assumed to be negligible by standard designers; the current standards employ a detached headform in helmet drop tests. A study on the full-scale and

detached head normal impacts of helmets has shown that the presence of the body increases the crushing distance of the helmet liner (Ghajari, et al., 2009). Therefore, it is probable to design a helmet that passes the standard test but its liner bottoms out when it is impact tested using the whole body. It has been proposed to increase the mass of the headform as a simple yet appropriate measure in order to take into account the effect of the body on the liner crushing distance and head linear acceleration.

The influence of the body on head rotational acceleration was studied in COST 327 by using a Hybrid III dummy. The helmeted dummy was drop tested onto the oblique abrasive anvil of the BS standard (which is the same as that of the ECE 22.05 standard) at 4.4 m/s, 5.2 m/s and 6 m/s impact speeds. In experiments, the dummy was horizontal and facing upward and the side of the helmet was impacted. The results were compared to the results of headform oblique impact tests. It was concluded that in order to access the head rotational acceleration by using a headform, the impact velocity should be slightly increased. One of the limitations of this study was using the Hybrid III dummy. This dummy was not designed for direct impacts. It has been criticized that the stiffness of the Hybrid III dummy neck in direct impacts is considerably higher than the human neck stiffness (Herbst, et al., 1998).

In this research, an FE model of the human body, THUMS, was employed to study the head/body interaction in helmet oblique impact tests. THUMS includes detailed and validated models of many of the biomechanically important parts of the human body, particularly the neck. Hence, it was believed that it will give better results (for the type of impacts considered in this study) compared to the Hybrid III dummy. It is attempted to quantify the influence of the body, on the head rotational acceleration in oblique impacts. A possible measure for including this effect in oblique impact test methods which use a detached headform is also discussed.

METHODOLOGY

HELMET FE MODEL: a commercially available helmet size K (58 cm) was chosen for this study. The helmet is called AGV-T2 throughout this text. The CAD files of the helmet parts, including foam parts and shell, were provided by the helmet manufacturer, AGV S.p.A. They were prepared for mesh generation and meshed by the Hypermesh software (HyperWorks, 2008). Tetrahedral elements with an average element size of 7 mm were used for the foam parts. The shell was meshed with quadrilateral shell elements with a 3 mm average element size. According to Cernicchi et al. (2008), this combination of element type and size for a helmet that has an expanded poly-styrene (EPS) liner and a composite shell results in converged linear acceleration of the headform in standard drop tests.

The helmet mesh was converted to LS-DYNA format and material properties were defined in this software (LS-DYNA, 2007). For the EPS foams, the Crushable Foam material model (MAT63) was employed. This material model requires the definition of the Young's modulus, Poisson's ratio and the compressive stress-strain characteristic curve of the foam. For a closed-cell polymeric foams, these properties are related to the relative density of the foam through semi-empirical equations explained in Cernicchi et al. (2008). Given the relative density of the helmet foam parts, these parameters were calculated and inserted into the relevant material cards. In Table 1, the properties of the main liner are presented.

The shell was formed of several layers of a unidirectional (UD) hybrid composite with an angle-ply lamination and UD glass/fibre and woven glass-fibre layers. Each layer was represented with a through-thickness integration point. At each integration point, the lamina was modelled with the Laminated Composite Fabric material model (MAT58) of LS-DYNA. MAT 58 is based on the principles of continuum damage mechanics developed by Matzenmiller at al. (1995). The elastic properties required for this material model are Young's moduli in fibre and matrix directions (E_{11} and E_{22}), one in-plane Poisson's ratio (e.g. v_{12}) and in-plane shear modulus (G_{12}). For failure, it is assumed that the lamina fails under tension and compression in both fibre and matrix directions and under in-plane shear. Therefore, the required parameters are tensile strength in the fibre direction ($\sigma_{11,ut}$), compressive strength in the same direction ($\sigma_{11,uc}$), tensile strength in the matrix direction ($\sigma_{22,ut}$), compressive strength in the same direction ($\sigma_{22,uc}$) and in-plane shear strength ($\tau_{12,u}$). The strains at the strength values were also required. The elastic and failure parameters of the hybrid composite were obtained through conventional mechanical tests at Imperial College London, which are presented in Table 1. For glass/fibre layers, the data available in open literature were employed.

Table 1 Material properties of helmet parts

Main liner									
	ρ (kg/m^3)			E (MPa)		υ		σ_y (MPa)	
	40			10.6		0.01		0.36	
Shell (hybrid composite)									
ρ	E_1	E_2	υ_{21}	G	$\sigma_{11,ut}$	$\sigma_{22,ut}$	$\sigma_{11,uc}$	$\sigma_{22,uc}$	$\tau_{12,u}$
1400	110	10	0.033	4.2	1700	49	400	130	90
					$\varepsilon_{11,ut}$	$\varepsilon_{22,ut}$	$\varepsilon_{11,uc}$	$\varepsilon_{22,uc}$	γ_u
					0.016	0.009	0.007	0.013	0.022

The FE model of the helmet was validated through simulating standard drop tests onto a flat anvil at impact points B (front), P (crown), R (rear) and X (side) as per ECE 22.05. The FE model of the helmet was positioned on a J size ISO headform considering the upper and lower vision filed angles defined in the standard. The impact points were also selected according to the definitions given in the standard. The helmeted headform was dropped onto a rigid wall at an impact speed of 7.5 m/s. During the impacts, the linear acceleration of the headform at its C.G. was recorded and compared to the experimental results. In this way, the validity of the model in normal impacts was assessed. It has been shown that in helmet oblique impacts, as long as the FE prediction of the normal force due to the foam compression is validated, the rotational acceleration of the headform is mainly dependent on the friction coefficients at the head/helmet and helmet/anvil interfaces (Mills and Gilchrist, 2008). For this study, realistic friction coefficients were selected, as explained later. In future, oblique impacts will be performed and simulated.

THUMS FE MODEL: an elaborate FE model of the human body called THUMS (Total Human Model for Safety) represented the human body in virtual impacts. The 50th percentile male pedestrian model of THUMS (THUMS, 2008) was available at LMU (Ludwig Maximilians University, Germany), which is one of the partners of the EU research training network, MYMOSA. This model was used during a short secondment at LMU. The model is composed of 145000 elements including 67800 solid, 74000 shell and 3200 beam elements. The THUMS' neck is modelled with seven vertebras (C1-C7), intervertebral disks, cartilages, ligaments and muscles. It is connected to the head and thorax through other ligaments and muscles. The neck and other parts of THUMS have been validated by simulating volunteer and cadaver experiments (Chawla, et al., 2005, Kitagawa, et al., 2006).

To enable measuring the head accelerations during drop test simulations, all deformable parts of the THUMS's head were switched to rigid, except the head skin. It is probable that shear of the skin can affect the head rotational acceleration. All rigid parts of the head were constrained to an inertia part located at the centre of mass of the head. Inertial properties of the head, excluding its skin, were calculated by using LS-DYNA and specified for this part.

FULL-SCALE OBLIQUE IMPACT: the AGV-T2 helmet was positioned on the head considering the upper and lower vision field angles, set in ECE 22.05. There was a small gap (about 2 mm) between the head and liner, which in real helmet is filled with the comfort foam. Previous studies have shown that the replacement of this foam with a gap in FE models does not affect the results (Aiello, et al., 2007, Cernicchi, et al., 2008). The chin strap was passed through the hole of the cheek foam and below the neck. In a pre-simulation, the chin strap was tightened with a 5 N force. Then, its nodes and elements were imported to the main model without pre-stress. Mills and Gilchrist (2008) found that the friction coefficient at the head/helmet and helmet/anvil interface can largely affect the head rotational acceleration. They tested bicycle helmets in oblique impacts by using a headform with a wig. When a friction coefficient of 0.2 was used at the head/helmet interface, FE simulations predicted the head rotational acceleration with good accuracy. In this study, the same value was used for this interface. The helmet/anvil friction coefficient was set to 0.4 in order to simulate impacts on the road surface.

In previous research on oblique impact testing of helmets, a helmeted headform was dropped at three different configurations to find the most severe one. Among them, the side impact caused largest

head rotational acceleration. In this impact, the vertical axis of the head body formed an angle of 20° with the surface of the anvil and the tangential velocity was normal to this axis in the rear-front direction. In our study, we chose the same impact configuration, as shown in Fig. 1. However, the body impact angle was increased to 30° because at lower angles, the shoulder of THUMS contacts the road surface before the head.

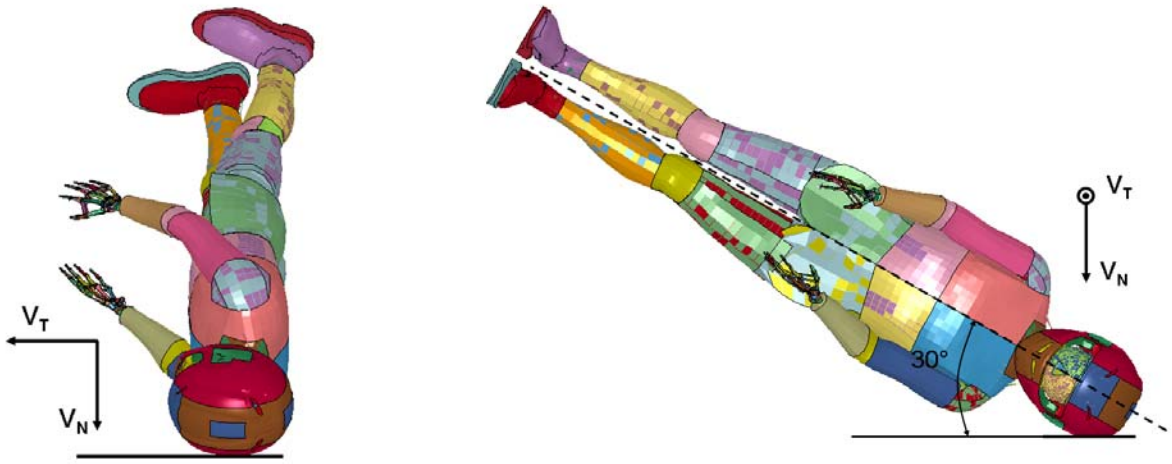

Fig. 1 Body impact angle and impact velocity components

HELMETED HEAD OBLIQUE IMPACT: As mentioned previously, the aim of this study was to assess the influence of the body on head rotational acceleration. Therefore, it was necessary to compare the full-scale oblique impacts with the same oblique impacts but without including the body. For this purpose, the head of THUMS was detached from the rest of its body and saved as a new model. This model also included part of the neck skin that supported the chin strap. The helmet was coupled with the head and the chin strap was tightened as explained before. The helmeted head was positioned at the side/30° (impact site/body impact angle) configuration. Hence, the new model was exactly the same as the full-scale oblique impact model except the body parts below the neck were not present.

RESULTS

HELMET VALIDATION IN NORMAL IMPACTS: the manufacturer of the helmet kindly provided one set of experimental data for comparisons with the FE results. However, to evaluate the repeatability of the experiments at least the results of three experiments at the same impact point are needed. This might explain some of the discrepancies between the FE and experimental results shown in Fig. 2. In this figure, resultant acceleration of the headform in plotted vs. time. The acceleration values are divided by the maximum FE acceleration. The results indicate that the model could predict the linear acceleration of the head with high accuracy, particularly for points P and X, which are close to the impact point of the side/30° configuration.

OBLIQUE IMPACT: for the oblique impacts several impact speeds were used. First, oblique impacts with a normal impact speed (V_N) of 5 m/s and tangential impact speeds (V_T) of 5 and 10 m/s were simulated. V_N=5 m/s represents the impact of a rider's head on the ground from a height of 1.3 m. As shown in Fig. 3, varying the tangential component of the impact velocity did not considerably change the linear acceleration of the head in both full-scale and detached head impacts. However, its influence on the rotational acceleration of the head was large. Fig. 4 shows the forces acting on the

helmet at its interface with the anvil. Around axis y and z, moments of the normal and tangential forces are in the same direction and around axis x only the normal force can produce a moment. The ratio F_T/F_N (presented in Table 2) could reach a maximum value of 0.4 (friction coefficient) when the tangential impact speed was large enough to cause sliding at the helmet/anvil interface. Hence, when the helmet was sliding on the anvil the moment was maximum and, consequently, the rotational acceleration was maximum.

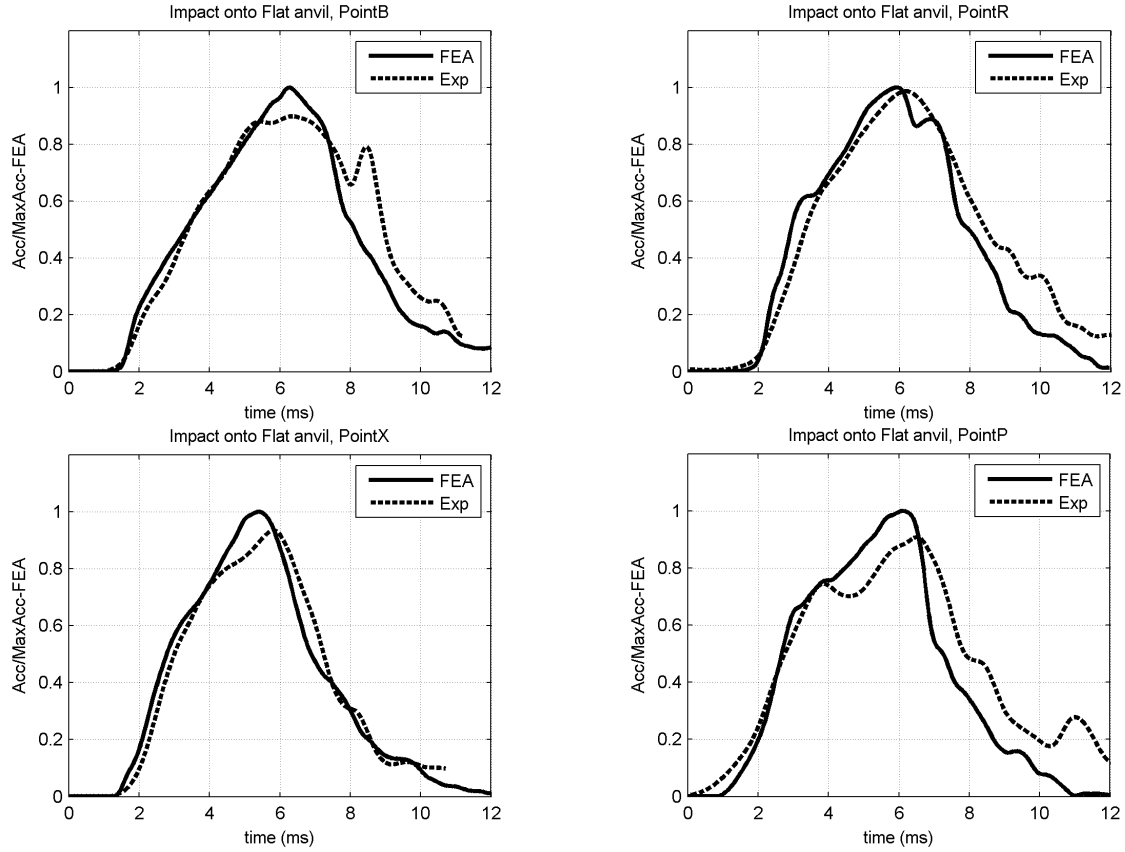

Fig. 2 Normal impact test results obtained by FEA compared to Experimental results

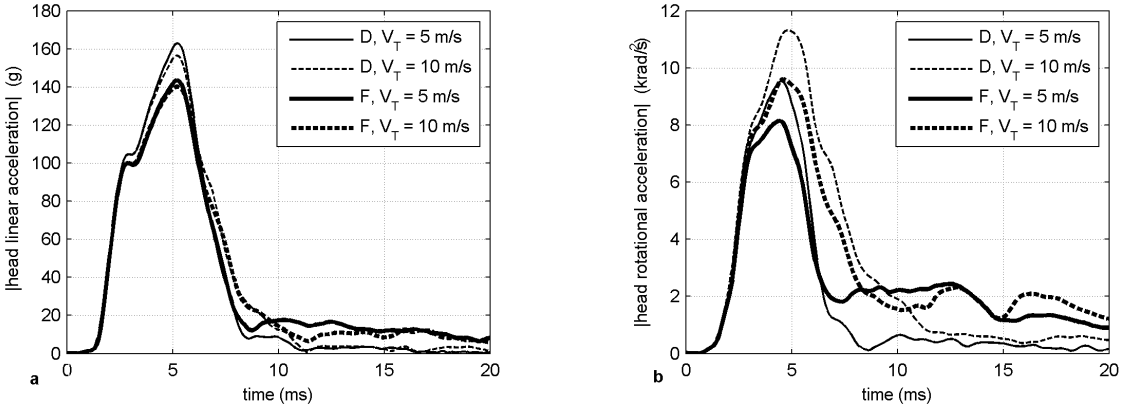

Fig. 3 – Head accelerations for detached head (D) and full-scale (F) oblique impacts, V_N=5 m/s

Second, the same impacts but at V_N=2.5 and 7.5 m/s were simulated. The latter is the impact speed adopted by the energy absorption test of the ECE 22.05 standard. As reported in Table 2, increasing

the normal component of the impact speed drastically increased the head linear acceleration as well as the rotational acceleration. For most of the impacts, the influence of this component of the impact velocity on the rotational acceleration was more than the effect of increasing V_T. In fact, as discussed before, when V_T was large enough to cause the helmet to slip on the anvil, F_T reached its maximum value and increasing V_T probably does not affect the tangential force. For instance, when V_N = 2.5 m/s for the detached head impact, increasing V_T from 5 m/s to 10 m/s hardly affected the head rotational acceleration since at V_T = 5 m/s the helmet was already sliding on the anvil. Conversely, increasing V_N caused more compression of the liner, thus higher normal forces.

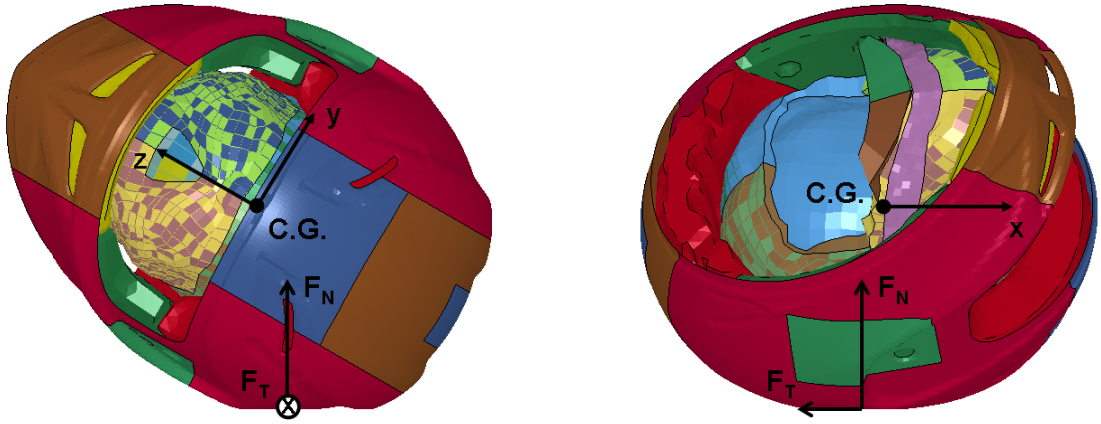

Fig. 4 Head attached frame (xyz) and helmet/anvil interface forces

The phenomena discussed so far were observed for both the detached head and the full-scale oblique impacts. In full-scale impacts, however, the resultant head accelerations were considerably lower (Fig. 3 and Table 2) as a result of the head/body interaction. The influence of the body on head linear acceleration and liner crushing distance was studied in another paper (Ghajari, et al., 2009). The aim of the present study was to investigate the influence of the body on head rotational acceleration. This influence can be shown mathematically as follows. The whole head can be assumed to be a rigid body because the scalp of the THUMS' head has a small mass compared to the mass of the other parts of the head and its deformation does not change the C.G. of the whole head. Therefore, the following equations can be used to relate the rotational behaviour of the head to the moments acting on it (Bedford and Fowler, 2002):

$$\mathbf{M}_h + \mathbf{M}_n = \mathbf{I}\boldsymbol{\alpha} + \boldsymbol{\omega} \times (\mathbf{I}\boldsymbol{\omega}) \quad (1)$$

where $\mathbf{M}_h$ is the helmet/head interface moment acting on the head, $\mathbf{M}_n$ is the moment applied on the head through the neck (both moments are about the C.G. of the head), $\mathbf{I}$ is the inertia matrix of the head at its C.G., $\boldsymbol{\alpha}$ is the vector of the head rotational acceleration and $\boldsymbol{\omega}$ is the vector of the head rotational velocity. The matrix and vectors in eq. (1) must be expressed in terms of their components in a body attached frame, such as the xyz frame introduced in Fig. 4. In the xyz frame, matrix $\mathbf{I}$ had three moments of inertia, I_{xx} = 216 kg.cm^2, I_{yy} = 262 kg.cm^2, I_{zz} = 199 kg.cm^2 and one non-zero product of inertia, I_{xz} = -41 kg.cm^2. $\boldsymbol{\alpha}$ and $\boldsymbol{\omega}$ were also known from FEA, but $\mathbf{M}_h$ or $\mathbf{M}_n$ could not be recorded in simulations. Since $F_{N,max}$ and $F_{T,max}$ of the full-scale impacts were very close to those of the detached head impacts (Table 2), it was assumed that $\mathbf{M}_h$ is equal to the head/helmet interface moment in the detached head impacts:

$$\mathbf{M}_h = \mathbf{M}_h^D = \mathbf{I}\boldsymbol{\alpha}^D + \boldsymbol{\omega}^D \times (\mathbf{I}\boldsymbol{\omega}^D) \quad (2)$$

where superscript *D* indicates quantities measured in the detached head impacts. Although these moments may not be exactly the same, the above assumption provided a reasonable approximation for $\mathbf{M}_h$ and $\mathbf{M}_n$.

Table 2 Results of the detached head and full-scale oblique impacts

Impact Type	V_N (m/s)	V_T (m/s)	$F_{N,max}$ (kN)	$F_{T,max}$ (kN)	F_T/F_N (r)[1]	$\|a\|_{max}$ (g)	$\alpha_{x,max}$ (krad/s^2)	$\alpha_{y,max}$ (krad/s^2)	$\alpha_{z,max}$ (krad/s^2)	$\|\alpha\|_{max}$ (krad/s^2)
Detached head	2.5	5	3.50	1.38	0.37 (0.995)	79	1.4	3.0	-4.6	5.5
		10	3.54	1.42	0.4 (1.000)	80	1.6	3.1	-4.6	5.7
	5	5	7.51	2.15	0.23 (0.938)	163	1.9	5.5	-8.2	9.5
		10	7.27	2.89	0.39 (1.000)	157	2.7	7.1	-9.4	11.3
	7.5	5	10.83	3.37	0.21 (0.928)	214	2.4	5.8	-10.2	11.2
		10	10.15	3.55	0.35 (0.985)	210	2.8	9.8	-12.5	15.2
Full-scale	2.5	5	3.50	1.37	0.35 (0.988)	73	2.2	2.4	-3.9	4.9
		10	3.66	1.46	0.40 (1.000)	74	2.5	2.5	-3.9	5.1
	5	5	7.69	2.14	0.24 (0.953)	144	3.9	3.7	-6.5	8.1
		10	7.43	2.96	0.39 (1.000)	140	4.5	5.5	-7.5	9.6
	7.5	5	10.93	3.37	0.23 (0.943)	185	5.4	4.2	-8.6	9.9
		10	10.25	3.57	0.35 (0.984)	183	5.4	7.4	-10.2	12.7
Modified detached head	5	5	7.41	2.14	0.25 (0.959)	160	3.5	4.4	-6.7	8.2
		10	7.28	2.90	0.40 (1.000)	154	4.6	5.2	-7.5	9.5
	7.5	5	10.70	3.37	0.23 (0.951)	215	3.7	4.8	-8.3	9.6
		10	10.04	3.57	0.36 (0.989)	207	5.1	7.7	-10.4	12.8

1) The slope of the line fitted to F_T vs. F_N data and the correlation coefficient.

The components of $\mathbf{M}_h$ and $\mathbf{M}_n$ are presented in Table 3 for various normal and tangential impact velocities. When a component of $\mathbf{M}_n$ has a sign opposite to the same component of $\mathbf{M}_h$, it indicates that the influence of the body was decreasing the magnitude of the same component of the rotational acceleration and vice versa. Therefore, the influence of the body was decreasing the magnitude of the acceleration about the y and z axes (rotations in the sagittal and axial planes respectively) but increasing the magnitude of the rotational acceleration about the x axis (rotation in the coronal plane). The value of $\alpha_{x,max}$ for all full-scale impacts was lower than the rotational acceleration threshold of 10 krad/s^2 (Margulies and Thibault, 1992). Nonetheless, Mills et al. (2009) used a helmet with a stiffer liner (60 g/l) in similar oblique impacts using a headform and found much higher values for $\alpha_{x,max}$ (for example $\alpha_{x,max}$ = 6.3 krad/s^2 when V_N = 5 m/s and V_T = 5 m/s, which is more than three times as high as $\alpha_{x,max}$ obtained in this study for the detached head impact at the same impact speeds). Consequently, the effect of the body on rotational acceleration components can be very important and probably should be considered in oblique impacts.

Table 3 Results of the full-scale oblique impacts

V_N (m/s)	V_T (m/s)	$M_{h,x}$[(1)] (N.m)	$M_{h,y}$ (N.m)	$M_{h,z}$ (N.m)	$M_{n,x}$ (N.m)	$M_{n,y}$ (N.m)	$M_{n,z}$ (N.m)	λ_x[(2)]	λ_y	λ_z
5	5	66	141	-169	55	-47	35	-0.26	0.27	0.31
	10	84	184	-196	50	-46	39	-0.20	0.26	0.31
7.5	5	77	149	-208	61	-58	39	-0.40	0.19	0.21
	10	93	252	-256	63	-72	48	-0.23	0.25	0.24

(1) Maximum values of moments are given in this table.
(2) For each modified inertia index, its value at the time of the peak of the corresponding rotational acceleration component is reported.

It was shown before that in order to take into account the effect of the body on head linear acceleration in normal headform drop tests, the mass of the headform should be increased (Ghajari, et

al., 2009). The analogous quantity in rotation is the inertia tensor. Hence, the aim was to find a modified inertia tensor for the detached head, $\mathbf{I}_m$, so that:

$$\mathbf{M}_h = \mathbf{I}_m \boldsymbol{\alpha} + \boldsymbol{\omega} \times (\mathbf{I}_m \boldsymbol{\omega}) \tag{3}$$

This equation results in three linear equations with six unknowns, namely I_{xx}, I_{yy}, I_{zz} , I_{xy} (= I_{yx}), I_{xz} (= I_{zx}) and I_{yz} (= I_{zy}). The head of THUMS has just one non-zero product of inertia, which is as small as less than 20% of its moments of inertia. It was assumed that this component is also zero. Therefore, using eq. (3), the three unknowns of $\mathbf{I}_m$ can be calculated as:

$$\begin{bmatrix} I_{m,xx} \\ I_{m,yy} \\ I_{m,zz} \end{bmatrix} = \begin{bmatrix} \alpha_x & -\omega_y\omega_z & \omega_y\omega_z \\ \omega_x\omega_z & \alpha_y & -\omega_x\omega_z \\ -\omega_x\omega_y & \omega_x\omega_y & \alpha_z \end{bmatrix}^{-1} \begin{bmatrix} M_{h,x} \\ M_{h,y} \\ M_{h,z} \end{bmatrix} \tag{4}$$

A set of dimensionless parameters were defined as:

$$\lambda_x = I_{m,xx}/I_{xx} - 1\,,\ \lambda_y = I_{m,yy}/I_{yy} - 1\,,\ \lambda_z = I_{m,zz}/I_{zz} - 1 \tag{5}$$

These parameters, which are called “modified inertia indices” in this text, were not constant versus time, as shown in Fig. 5. However, to modify the inertia matrix of the head, one value should be selected for them. As the main aim is to modify the peak of the rotational acceleration components, the values at the time of the peak of the rotational acceleration components were chosen. The modified inertia indices were calculated for different normal and tangential velocities, which are presented in Table 3. This table shows that the indices were dependent on the normal and tangential components of the impact velocity.

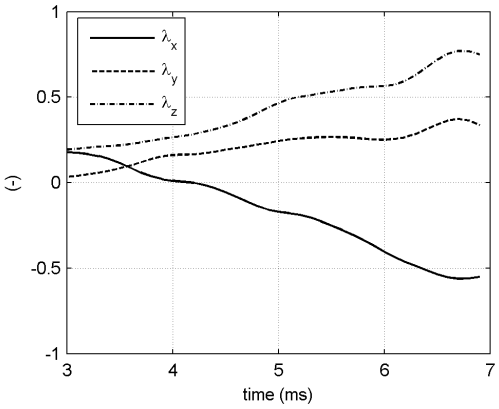

Fig. 5 Modified inertia indices, V_N = 5 m/s and V_T = 10 m/s

To verify the assumptions made to calculate a modified inertia tensor, the head was modified by replacing its $\mathbf{I}$ with $\mathbf{I}_m$ and the same oblique impacts were simulated. To calculate $\mathbf{I}_m$, the modified inertia indices corresponding to V_N = 5 m/s and V_T = 10 m/s were used. The impact results are given in Table 2. As it was expected, the best prediction of the head rotational acceleration components of the full-scale impacts were found when V_N = 5 m/s; the maximum discrepancy was about 19% for $\alpha_{y,max}$ when V_T = 5 m/s. The worst prediction was made when V_N = 7.5 m/s and V_T = 5 m/s. This is due to the fact that the relevant indices for these velocities were up to 50% different from those used to calculate $\mathbf{I}_m$ (Table 3). Despite the dependency of the indices on the impact speed, they can be used in an oblique impact test method because in test methods usually one value is set for the impact speed. The results show that the modified head could predict the head rotational acceleration components with a

high accuracy for the impact speeds for which the indices were chosen. There is also good agreement between resultant rotational accelerations of the full-scale impacts and those predicted in detached head impacts for all impact speeds, as reported in Table 2 and shown in Fig. 6.

The second peak of the head rotational acceleration in full-scale impacts, shown in Fig. 6, was due to the neck energy release. This energy was accumulated in the neck muscles during the crushing of the helmet from 0 ms to about 5 ms. When the helmet rebounded and the anvil/helmet forces (F_N and F_T) dropped towards zero, the constraints on the head were removed and the release of the elastic energy accumulated in the neck resulted in the second peak of the head rotational acceleration. This phenomenon cannot occur in detached head impacts. This second peak is also recognizable in Fig. 3 for the full-scale impact at V_N = 5 m/s and V_T = 5 m/s and 10 m/s but its value is approximately half of that when V_N = 10 m/s. It can be concluded that the value of this peak was mainly affected by V_N rather than V_T.

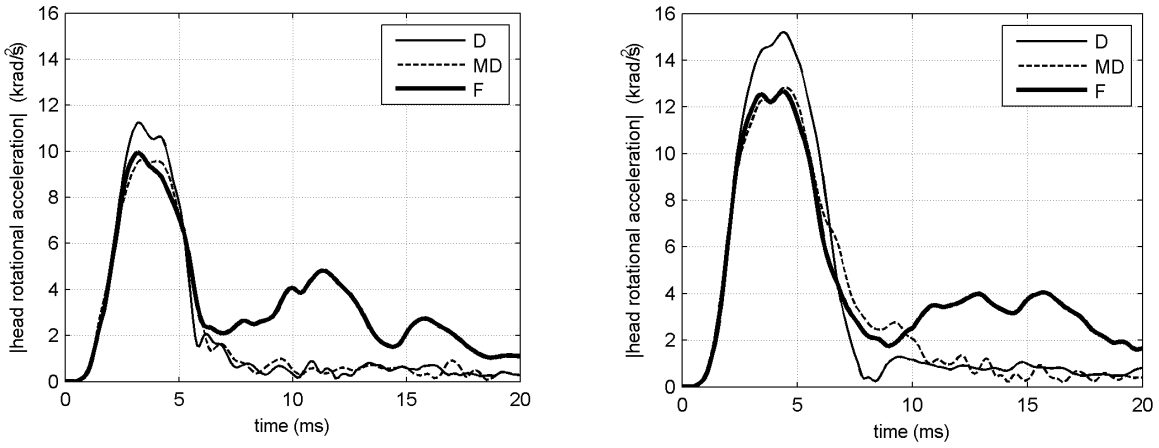

Fig. 6 Head acceleration for detached head (D), modified detached head (MD) and full-scale (F) oblique impacts; V_N = 7.5 m/s and a) V_T = 5 m/s , b) V_T = 10 m/s

Comparing the $|a|_{max}$ of the detached head and the modified detached head results (Table 2), it can be inferred that $|a|_{max}$ was independent of the changes in the inertia matrix of the head (within the ranges reported in this study). To take into account the influence of the body on $|a|_{max}$, the mass of the head should be increased, as shown by Ghajari et al. (2009). By using a Hybrid III dummy and its detached head in normal drop tests at the front site, they found that the head mass should be increased by 48%. However, the authors believe that this value has been overestimated due to the extremely stiff neck of the Hybrid III dummy.

DISCUSSION

The influence of the body on head rotational acceleration has been investigated in COST (2001) by oblique impact testing a helmeted Hybrid III dummy. The head resultant rotational acceleration was found to be higher than similar tests but by using a Hybrid II headform. It was interpreted as the influence of the body, which increases one component of the rotational acceleration. Similar phenomenon was observed in our simulations for α_x, but its increase was not so large to overcome the inverse effect of the body on other two components of the rotational acceleration. The results obtained in COST tests might be far from reality because they used a Hybrid III dummy; this dummy has a neck that was designed for studying injuries of car occupants in frontal impacts. In this study we used the THUMS human body model. Even though the cervical spine of THUMS has only been validated against inertial head loading scenarios (Chawla, et al., 2005, Kitagawa, et al., 2006), we believe that using a human body model with a correct anatomical representation of the neck provides more realistic insight into the head/body coupling than the Hybrid III dummy.

The heads used in this study for the full-scale and detached head impacts were the same. In this way, the only difference between these two types of simulations was the presence or absence of the rest of the body and the comparison between their results revealed the influence of the body but for the THUMS head. The inertial properties of the THUMS head are slightly different from those of the headforms that have been used for experimental oblique impacts, such as the Hybird II and Ogle-Opat headform (COST327, 2001, Mills and Gilchrist, 2008). The moments of inertia of an Ogle-Opat headfrom were reported I_{xx} = 199 kg.cm^2, I_{yy} = 237 kg.cm^2 and I_{zz} = 172 kg.cm^2, which are respectively 8%, 10% and 14% lower than those of the THUMS head. Nonetheless, the modified inertia indices proposed for modifying the headform's inertia tensor (given I_{xz} = 0), were dimensionless parameters. They define the percentage of the increase or decrease in the head's moments of inertia. Therefore, they may be used to calculate the modified inertia matrix of a test headform in order to include the effect of the body on rotational acceleration components of the head. It should be noted that the indices are specific to the simulated impact configuration. In future, they should be calculated for other impact configurations.

The head rotational acceleration is believed to be an important cause of head injuries (Gennarelli, 1983, Holbourn, 1943, Margulies and Thibault, 1992). Nevertheless, the aim of the oblique impact test of current standards (BS6658, 1985, UNECE22.05, 2002) is to assess the force caused by friction at the helmet/anvil interface, $F_{T,max}$. In COST 327, it was shown that there is a strong linear relationship between $F_{T,max}$ and $|\alpha|_{max}$. However, this relationship was found for a single impact site. Mills et al. (2009) showed that there is no correlation between these parameters when a range of impact sites were considered. They also found that for a single site, the slope of the line fitted to the $F_{T,max}$ vs. $|\alpha|_{max}$ data was dependent on the helmet used. It was concluded that $F_{T,max}$ cannot be a surrogate for $|\alpha|_{max}$. This is the reason why in this study, we focused on the rotational acceleration of the head and not on other surrogates. These findings suggest that in an effective oblique impact test, the rotational acceleration of the head should be directly measured and the effect of the body should be included by, for instance, modifying the inertial properties of the headfrom as explained in this paper.

Current standards do not have an oblique impact test or if they have V_N is very low. While values of V_N more than 5 m/s are typical of severe accidents, in the current oblique impact test methods V_N < 2.6 m/s. This component of the impact velocity affects the liner crushing distance and consequently the normal force on the head. Mills et al. (2008) reported that the moment of a normal force not passing through the C.G. of the head contributed to as much as 40% of the head rotational acceleration in a bicycle helmet oblique impact. As shown before, for V_T = 10 m/s the helmet was sliding on the anvil. Sliding of the helmet produces the maximum tangential force, which in the simulated impact configuration caused maximum rotational acceleration for a given V_N. Therefore, at V_N = 5 m/s and V_T = 10 m/s the performance of helmets would be evaluated in severe but more probable conditions. However, it is very expensive to adapt test laboratories to test helmets at large impact velocities due to their height limitations. A reasonable proposal for velocity components of an effective oblique impact test could be V_N = 5 m/s and V_T = 8.5 m/s. This can be achieved by dropping the helmeted headform onto an anvil inclined at 30° to the vertical, from a height equivalent to an impact velocity of 10 m/s (which is equal to the impact velocity of the oblique impact test of the BS6658 standard).

The FE model of the helmet used in this study was only validated against normal impacts. In future, it will be validated against oblique impact tests. As mentioned before, the THUMS FE model represents the anatomical structures of the (cervical) spine much better than for instance a dummy, but it has not specifically been developed for the kind of impacts studied in this paper. Therefore, there is a need for evaluating the performance of the THUMS' head and neck when its head is subjected to direct impacts.

CONCLUSIONS

A commercially available helmet was modelled in LS-DYNA and oblique impact tested by using the THUMS human body model. The results were compared with the results of the same impacts but by using the detached head of THUMS to exclude any effect bar the presence of the rest of the body. For the studied impact configuration, it has been shown that the presence of the body influences the head rotational acceleration components considerably. In one case, it increased one component of the acceleration by 40%. Overall, it decreased the resultant rotational acceleration of the head by up to 18%.

On the basis of the equations of general three-dimensional motion of a rigid body, the moments acting on the head through the neck were estimated. These moments affect the head rotational acceleration in full-scale impacts compared to detached head impacts. It has been shown that a simple yet appropriate measure to account for them in detached head oblique impacts could be modifying the inertia matrix of the head. The modified inertia indices were calculated for a specific impact configuration and various impact velocities.

Including a severe oblique impact test in standards causes the engineers to optimize helmets for more realistic test conditions. A reasonable oblique impact test, which induces rotational accelerations typical of severe impacts, could be dropping a helmet, positioned on a modified headform, at an impact velocity of 10 m/s onto a flat anvil inclined at 30° to the vertical.

ACKNOWLEDGEMENTS

The work presented in this paper was completed within the research training network MYMOSA funded by the Marie Curie fellowship of the 6th framework programme of the EU under contract no. MRTN-CT-2006-035965. The authors would like to thank Dainese S.p.A. for providing the CAD files of the helmet.

REFERENCES

1. Aiello, M., Galvanetto, U., and Iannucci, L., Numerical simulations of motorcycle helmet impact tests. International Journal of Crashworthiness 12, 2007, 1-7.
2. Bedford, A., and Fowler, W. L., Engineering mechanics : dynamics study pack. Prentice Hall, Upper Saddle River, NJ, 2002.
3. BS6658, Protective helmet for vehicles users, British Standards Institution, 1985.
4. Cernicchi, A., Galvanetto, U., and Iannucci, L., Virtual modelling of safety helmets: practical problems. Int. J. of Crashworthiness 13, 2008, 451-467.
5. Chawla, A., Mukherjee, S., Mohan, D., and Jain, S., Validation of the cervical spine model in THUMS. 19th International Technical Conference on the Enhanced Safety of Vehicles, Washington D.C., US, 2005.
6. COST327, Motorcycle safety helmets, final report of the action. European Communities, Belgium, 2001.
7. Gennarelli, T. A., Head injury in man and experimental animals: clinical aspects. Acta neurochirurgica. Supplementum 32, 1983, 1-13.
8. Ghajari, M., Caserta, G. D., and Galvanetto, U., Comparison of safety helmet testing standards. Imperial College London, London, 2008.
9. Ghajari, M., Galvanetto, U., and Iannucci, L., Influence of the body on kinematic and tissue level head injury predictors in motorcyclists accidents. IRCOBI, York, UK, 2009.
10. Herbst, B., Forrest, S., Chng, D., and A. Sances, J., Fidelity of anthropometric test dummy necks in rollover accidents. 16th International Technical Conference on the Enhanced Safety of Vehicles, Windsor, Canada, 1998.
11. Holbourn, A. H. S., Mechanics of head injuries. Lancet 242, 1943, 438-441.
12. HyperWorks, 9.0 Release. Altair, 2008.
13. Kitagawa, Y., Yasuki, T., and Hasegawa, J., A study of cervical spine kinematics and joint capsule strain in rear impacts using a human FE model. Stapp Car Crash J. 50, 2006, 545-566.
14. LS-DYNA, Version 971. Livermore Software Technology Corporation, 2007.
15. Margulies, S. S., and Thibault, L. E., A Proposed Tolerance Criterion for Diffuse Axonal Injury in Man. J. Biomech. 25, 1992, 917-923.
16. Matzenmiller, A., Lubliner, J., and Taylor, R. L., A Constitutive Model for Anisotropic Damage in Fiber-Composites. J. Mech. of Mater. 20, 1995, 125-152.
17. Mills, N. J., and Gilchrist, A., Finite-element analysis of bicycle helmet oblique impacts. Int. J. Impact Eng. 35, 2008, 1087-1101.
18. Mills, N. J., and Gilchrist, A., Oblique impact testing of bicycle helmets. Int. J. Impact Eng. 35, 2008, 1075-1086.
19. Mills, N. J., Wilkes, S., Derler, S., and Flisch, A., FEA of oblique impact tests on a motorcycle helmet. Int. J. Impact Eng. 36, 2009, 913-925.

20. Nightingale, R. W., McElhaney, J. H., Richardson, W. J., and Myers, B. S., Dynamic responses of the head and cervical spine to axial impact loading. Journal of Biomechanics 29, 1996, 307-318.
21. Richter, M., Otte, D., Lehmann, U., Chinn, B., Schuller, E., Doyle, D., Sturrock, K., and Krettek, C., Head injury mechanisms in helmet-protected motorcyclists: Prospective multicenter study. Journal of Trauma-Injury Infection and Critical Care 51, 2001, 949-958.
22. THUMS, AM50 Pedestrian Model: Version 3.0-080225. TOYOTA Central R&D LABS, 2008.
23. UNECE22.05, Uniform provisions concerning the approval of protective helmets and of their visors for drivers and passengers, United Nations, 2002.